

Distributed control of a multi-agents magnetic levitation system

Antonio Minonne, Anna Paola Musio, Samuele Paone, Salvatore Pappalardo
s280095, s281988, s287804, s281621

Introduction

This project implements a system of 6 distributed magnetic levitation systems, linearized in an equilibrium point. We applied the theory as described in chapter 3 of the book [Cooperative Control of Multi-Agent Systems](#). In the first, section we briefly explain the simulink model and the code used for the simulations, as well as the other files of the project. The second section briefly analyzes the performance of different network structures in terms of Global Disagreement Error on the output of the systems. The third section is dedicated to the comparison between the performances of using either a distributed observer or a local one. Finally, the last section explains a slightly different architecture that works for our systems, even though we could not prove the general case.

Files arrangement

For information about the simulink and matlab implementation, please refer to the file [README.md](#).

There are 4 types of files.

stable_ prefix

These files are related to the theory as seen in class lessons. Each magnetic levitator is controlled using the pole-placement method. In order to do that, since the state of the system is not measurable, we needed to add an observer which provided the state, given its output.

The “placed poles” are chosen in order to impose a specific trajectory to the leader.

Each other agent is virtually connected to all the other agent. Whether the connection actually exists depends on the adjacency matrix of the graph.

Each agent also has an observer as explained by the theory, which serves the purpose of estimating the controlled state to calculate ϵ . This kind of architecture is a bit redundant, since we already have an observer, but it is necessary since the two observers estimate different states, specifically: the internal one estimates the actual state of the maglev, the external one estimates the state of the **controlled maglev**.

alternative_ prefix

These files are relative to the *slightly different* architecture as mentioned above. For further information, read the last section of this document.

Regarding the files, they are an almost exact copy of the **stable_** files.

metric_prefix

These files contain useful functions needed to score the performance of the system.

The file `metrics.txt` contains a description of each implemented metric.

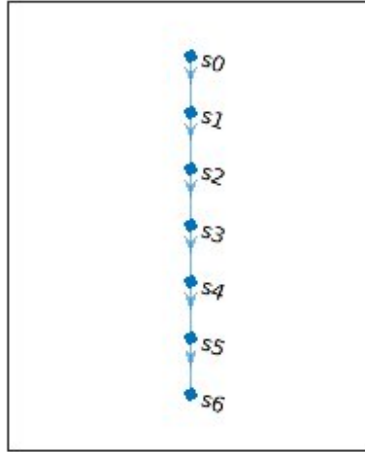
Network structure analysis

If no otherwise specified, the convergence times correspond to the time t^* such that the error

$$|y_i(t) - y_0(t)| < 100 \mid t \geq t^*,$$

Chain structure

We performed several experiments with chain structure. In the cases where there was not a forward edge between follower nodes, or loop structures in the chain.



Observation 1

In a chain structure network, where there aren't forward edges among follower nodes or loop structures in the chain, if we have nodes i and j , and node j is the successor nodes of node i in the chain, and all the weights associated with the edges are equal:

$$Tc_j > Tc_i$$

where:

- Tc_j is the convergence time of node j
- Tc_i is the convergence time of node i

In the following, we report the table of the convergence times for each nodes.

Node i	Convergence time
1	11.2141
2	12.0108
3	12.4916
4	12.8382
5	13.1102
6	13.3334

We went forward with the experiments changing the weights associated with the edges, with the same network topology described previously. We have noticed that *Observation 1* is still true.

Observation 2

In a chain structure, like the one described in *Observation 1*, if node j is the successor of node i , and $w_{(j,i)}$ is the weight associated with the edges (i,j) , then,

$$w_{(j,i)} \rightarrow \infty \Rightarrow Tc_j \rightarrow Tc_i$$

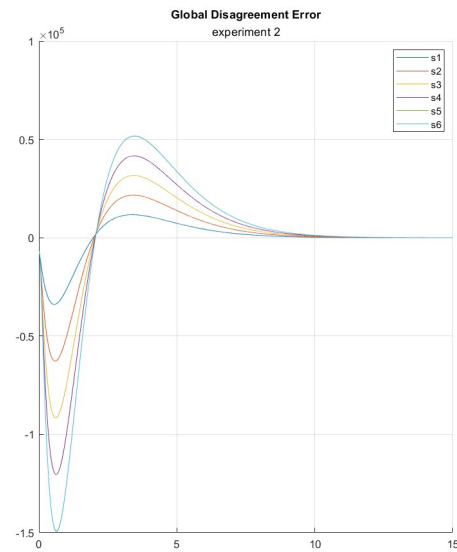
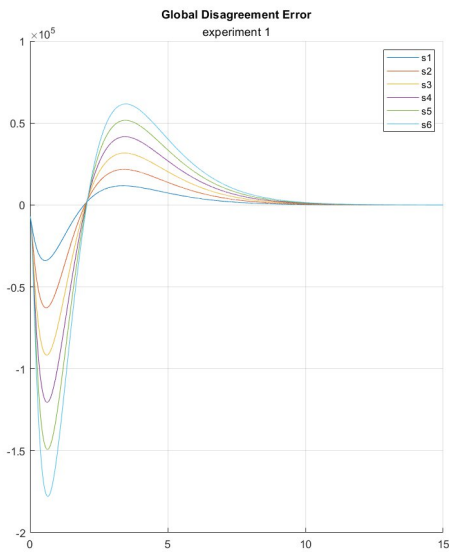
where:

- Tc_j is the convergence time of node j
- Tc_i is the convergence time of node i

In fact, in our example, increasing the weight associated with the edges (5,6) up to 100, leaving all others weight in the network equal to 1, we can notice that Tc_6 approaches Tc_5 , without ever going under it. From the table shown in the following we can see how, with this new configuration of weights, $Tc_6 \simeq Tc_5$.

Node i	Convergence Time
1	11.2141
2	12.0108
3	12.4916
4	12.8382
5	13.1102
6	13.1122

We can have a better idea of the impact that the weights have on convergence time of a generic node i , looking at its global disagreement error (GDE), in the following we report the trend of GDE for each node in experiment one and two.



We can see that the trends of GDE for each node in the experiment one are equidistant from each other, because all weights are set to 1. On the other hand in the experiment 2 we can notice that the GDE trend of nodes 6 collapses on the GDE trend of node 5. The reason for this behavior is that, for this experiment we set $w_{6,5} = 100$.

After the experiments described previously, we changed the network topology, by adding a forward edge. From that experiment we noticed that the node, that receive the information thanks to the forward edge, reduces its convergence time in according to some sort of rule.

Observation 3

If in a chain structure, like the one described previously, we add a forward edge from node i to node j , the improvement on convergence time of node j depends on: -

$$d_{li} = \sum_{k=1}^i \frac{1}{w_{(k,k-1)}}$$

The sum of the weights's reciprocals associated with the edges among leader node and i

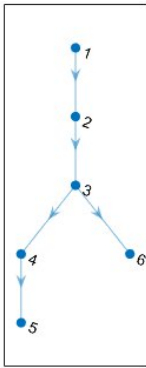
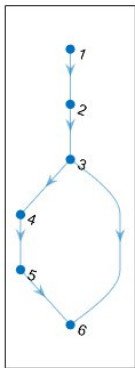
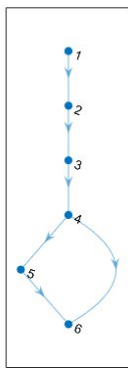
$$d_{ij} = \sum_{k=i}^j \frac{1}{w_{(k,k-1)}}$$

- *The sum of the weight's reciprocals of the weights associated with the edges among i and j in the original chain structure*

$$d_{fij} = \frac{1}{w_{(j,i)}}$$

- *The weight's reciprocal associated with the forward edge (i,j)*

To better understand the behavior of node convergence , we tried different configuration of chain structures by adding for every try different edges.

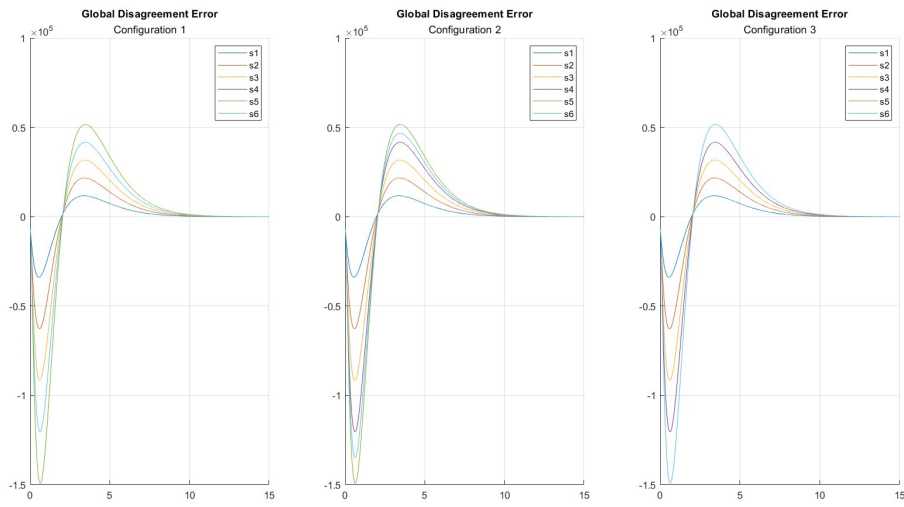
Configuration 1	Configuration 2	Configuration 3
		

In this experiment all the weights are set to one. In fact, the aim now is to study the convergence time for different networks topology. In particular, we focus our attention on

node 6 because we modify only the input degree of this node and the nodes from where it gets information. The results for this experiments are shown below.

Time Convergece table

Node	Convergence time		
	Configuration 1	Configuration 2	Configuration 3
1	11.2141	11.2141	11.2141
2	12.0108	12.0108	12.0108
3	12.4916	12.4916	12.4916
4	12.8382	12.8382	12.8382
5	13.1102	13.1102	13.1102
6	12.8382	12.9828	13.1102



We noticed that the first configuration collapses to a binary tree structure, (which will be discussed better later), in fact the behavior on nodes 6 is equal to the behavior of node 4.

In the second configuration the nodes 6 converges with greater delay respect the first configuration, despite we leave the forward edge from node 3 to node 6. But node 6 converges before node 5. This makes us suspect that the information that node 6 taken by node 5, increases the convergence time.

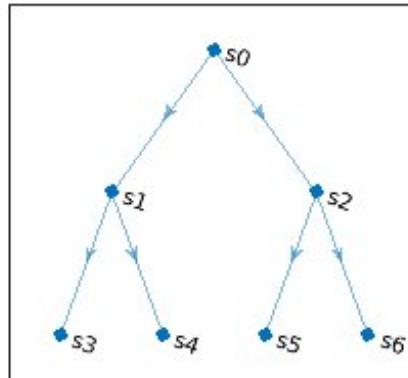
In the third configuration node 6 take information from node 4, a node that is farer from the leader than nodes 3 and we noticed that the convergence time of node 6 increases, exceeding the convergence time of node 5.

Experimental rule

In a chain configuration structure, if all edges have the same weights, when we apply a forward edge from node i to node j , decreasing d_{li} , d_{ij} and d_{fij} , we increase the improvement in terms of convergence time

Tree structure

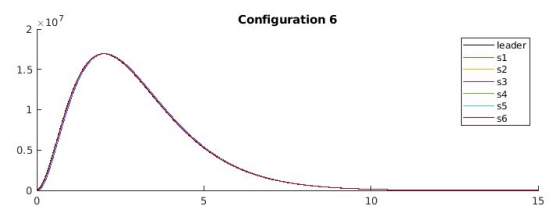
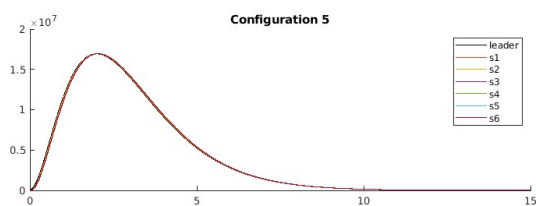
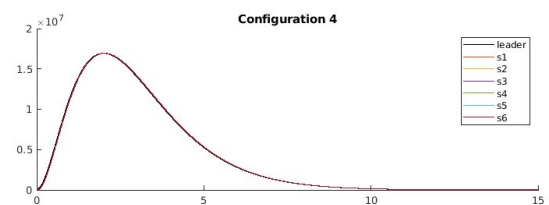
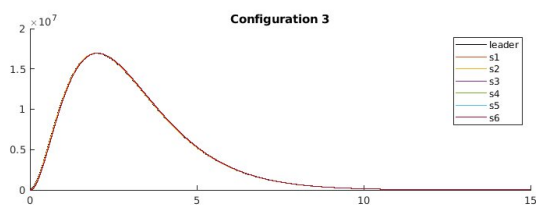
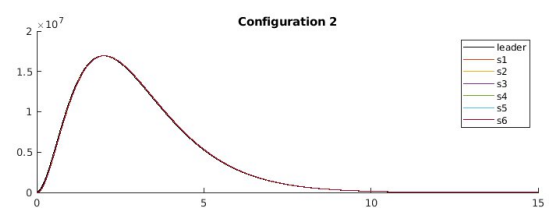
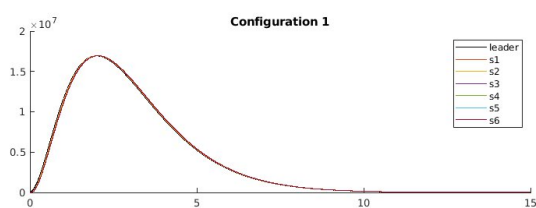
The tree structure is shown in the following figure



We analyzed 6 different network configurations with different weights. Those are summarized in the following table.

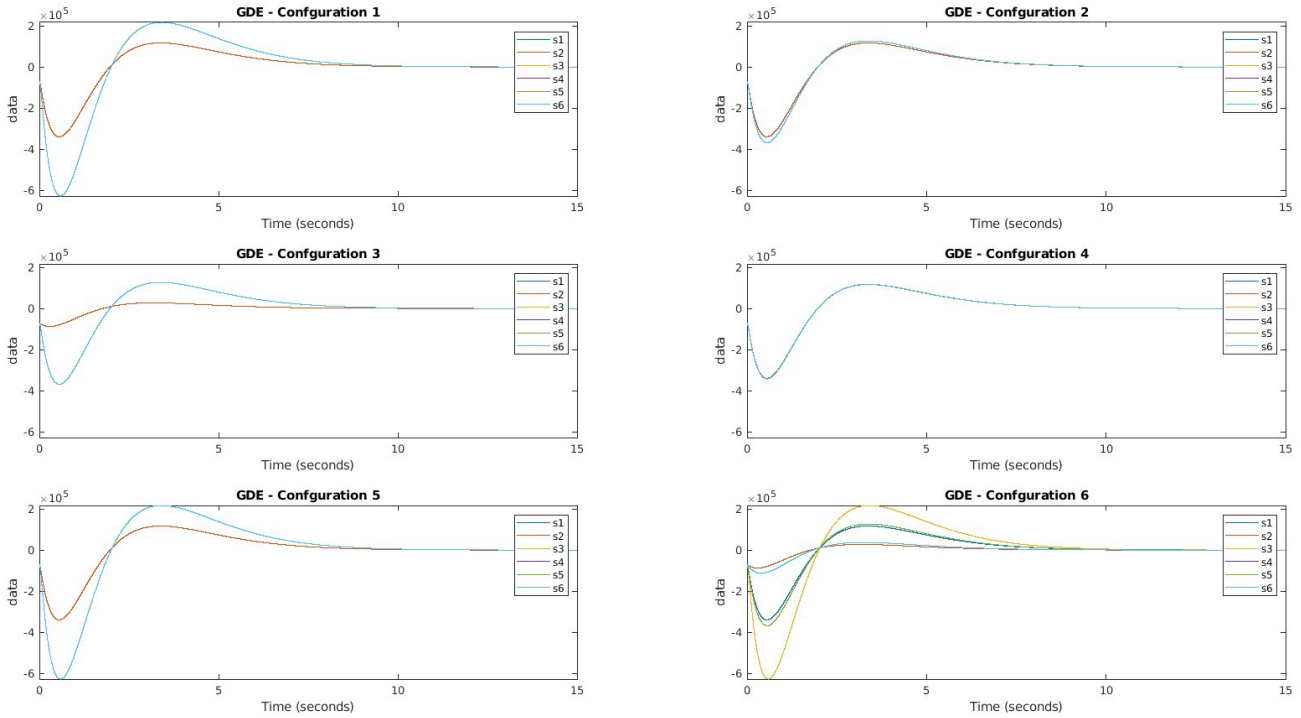
n	Configuration	0->1	0->2	1->3	1->4	2->5	2->6
1	Equal weights at 1	1	1	1	1	1	1
2	Increasing weights	1	1	10	10	10	10
3	Decreasing weights	10	10	1	1	1	1
4	Same convergence time	1	1	100	100	100	100
5	Big equal weights	1e10	1e10	1e10	1e10	1e10	1e10
6	Asymmetric weights	1	10	1	10	1	10

The following figures illustrates the step response and the **global disagreement error (GDE)** with respect to the output of each system.



The first notable thing is that the convergence time does not depend on the value of the weight itself, but rather there seems to exist a relationship which quantifies the similarity of the behaviors and the convergence times.

Indeed, when comparing Configuration 1 and Configuration 5 (in which the difference is only the magnitude of the weights) we can clearly see that they have the same behavior even though completely different weights. On the other hand, Configurations 1, 2 and 4 have increasingly similar behavior, with the slower nodes matching the behavior of the faster ones.



Another important aspect to underline is the *class of convergence*. In the context of the first five configurations, only two curves are clearly visible. This happens because nodes s1 and s2 converge at the same time: they *belong to the same class*. The same can be said for nodes s3, s4, s5 and s6.

Although there seems to be a simple relationship, the next example demonstrates things are more complicated.

In Configuration 6 the tree is *unbalanced* and this fact heavily modify the behavior. The table shows the convergence times of the nodes for this configuration in increasing order:

node	convergence time
2	9.13
6	9.62
1	11.21
4	11.32
5	11.32
3	12.01

Note: This convergence times are calculated with a threshold of 1000.

It seems that these times follow the next constraint

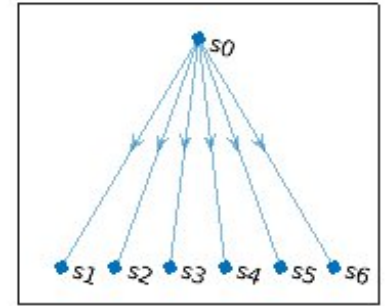
$$T_i \propto \Omega_i, \text{ where } \Omega_i = \sum_{j=1}^d \frac{1}{w_j}$$

It is clear that the bigger the weight and smaller the depth, the faster the convergence. Node s2 has the 1 and weight 10, thus is the first to converge. The second place belongs to s6 which is a direct child of s2 and has again a weight of 10. Then, s1 converges and it has depth 1, but weight 10 and next we find s4, which is a direct child of s1 and has weight 10. Finally s2 is a direct child of s2 but has weight 1 and s3 has depth 2 but weight 1.

To further investigate the relationship with the depth, we experimented with another network structure, which is presented in the following section.

Dictator structure

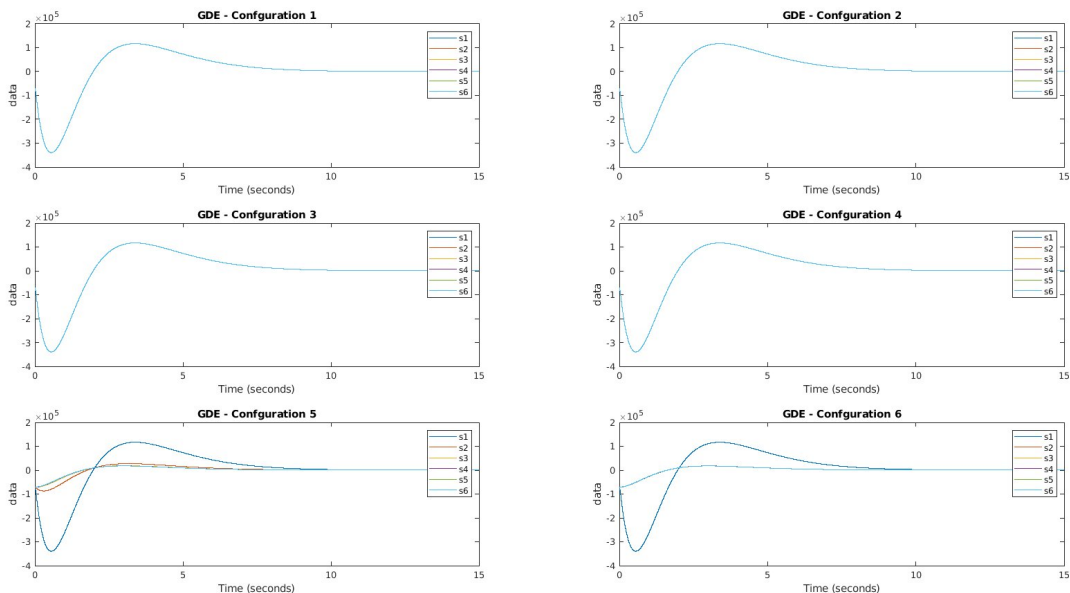
We called “dictator” the structure in which each agent is directly connected with the leader and no-one else. The following figure illustrate the concept.



We used 6 configurations once again. They are listed below.

n	Description	0->1	0->2	0->3	0->4	0->5	0->6
1	Equal weights at 1	1	1	1	1	1	1
2	Equal weights at 1e3	1e3	1e3	1e3	1e3	1e3	1e3
3	Equal weights at 1e6	1e6	1e6	1e6	1e6	1e6	1e6
4	Equal weights at 1e9	1e9	1e9	1e9	1e9	1e9	1e9
5	Powers of 10	1	10	10 ²	10 ³	10 ⁴	10 ⁵
6	Powers of 1000	1	1e3	1e6	1e9	1e12	1e15

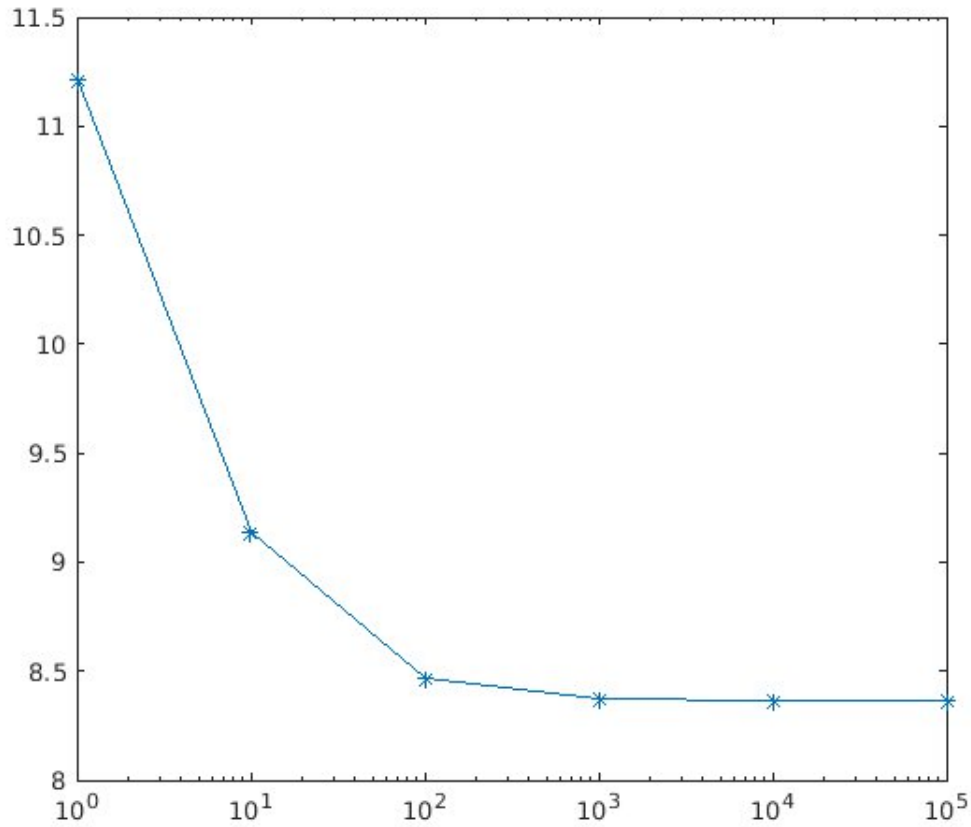
The error are as illustrated in the following image



The first remarkable point is that Configurations 1, 2, 3 and 4 have the same behavior. This results, paired with the previous one, indicates that the **convergence time is the same when all the weights are the same**.

The last two example shows a relationship of the type $T_i \propto \frac{1}{w_i}$, where T_i denotes the convergence time of node i and w_i is the pinning gain for the same node.

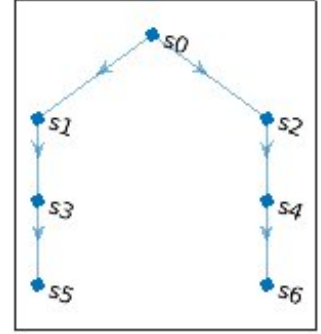
Configuration 5 is interesting because it shows us what seems to be a super-exponential relationship between the weights and the convergence time. The next figure shows the semilogx plot of the convergence time with respect to the weights.



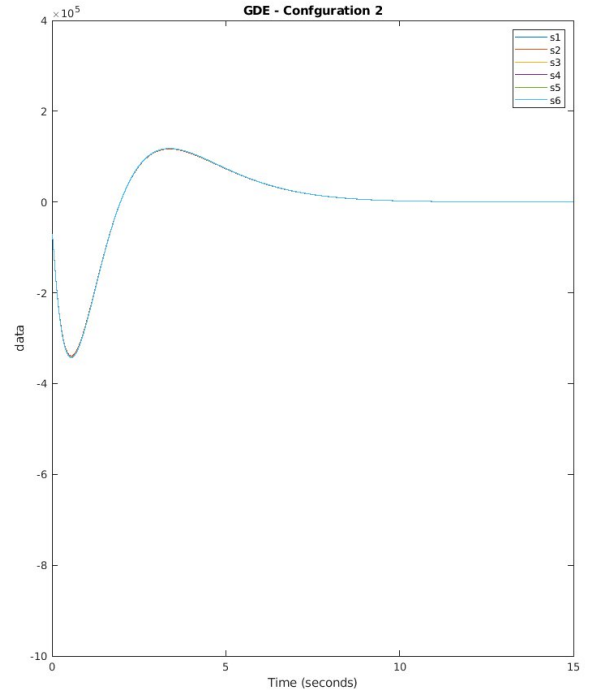
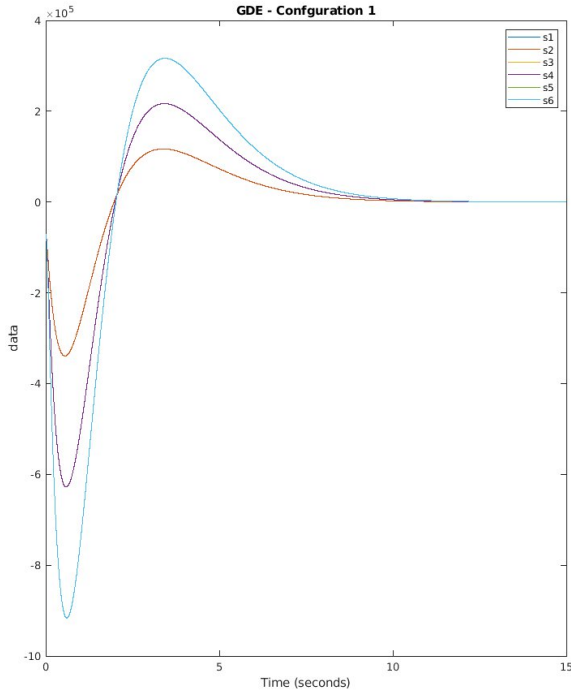
Double-chain structure

The double-chain structure is a tree in which the leader has 2 childs and each child has only one child, as follows.

Analyzing this structure and pairing the results with the *single-chain* structure, it appears very clear that there is inverse proportional relationship between the depth and the convergence time. This result corroborates the unknown relationship of the graph structure, which should be general for *one-way* networks.



$$T_i \propto \frac{1}{d_i}$$

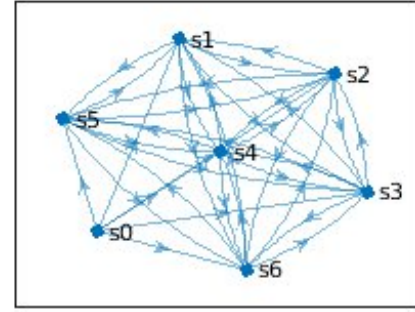


And also that exists some kind of relationship between the convergence time and the ratios of the weights along the chain.

Complete structure

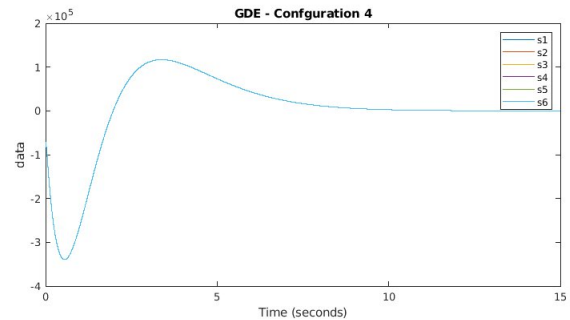
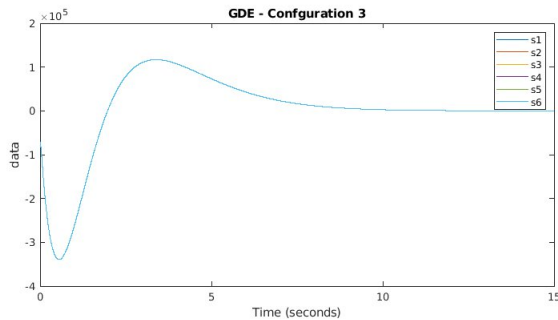
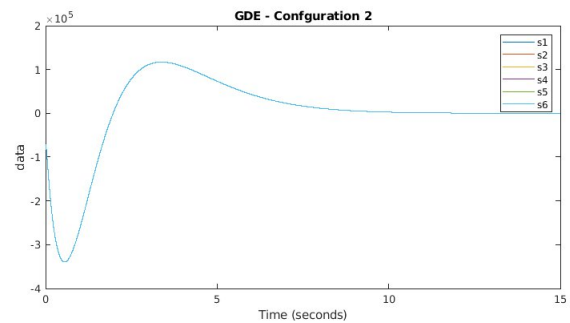
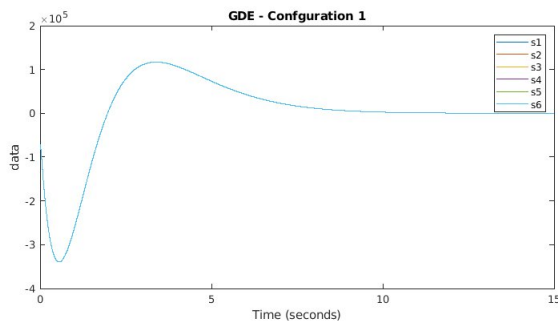
The complete structure is shown in the following figure.

In this structure, each node communicates with each other node. The leader is connected to every agent. This structure is peculiar, since it produces always the same results, no matter what weights are chosen. In the following figure, we show the GDE for four different configurations.



n	description	weights
1	Equal weights	1
2	Equal weights	100
3	Random weights 1	random
4	Random weights 2	random

This happens because each node receives always the same informations, even though with different weights. The peculiarity is that the informations kind of average always out , thus producing always the same results.



Although this is the most reliable structure (both in terms of performance and reliability) it also is the most expensive, needing to connect every node six times.

Final considerations

Summing up the conclusion we can say that if:

1. the graph is acyclic and
2. at least one weight is different from the others

then the following relationship holds

$$T_i \propto \Omega_i, \text{ where } \Omega_i = \sum_{j=1}^d \frac{1}{w_j}$$

While, if the weights are all the same, the convergence time only depends on the network topology.

Although we weren't able to find some clear relationship between the convergence times and the network structure, we are pretty sure this same problem was already studied in the past. References like [1](#) seem to have studied this problem. Also we should be able to apply [Flow network theory](#) to study this problem.

In the next section we discuss the chosen network, in terms of cost and performance.

Comparison between architectures

In order to perform these tests we chose the tree structure because we took into consideration two factors: the structure generality and the feasibility in terms of applications domain, i.e. the maglev. The dictator and full-graph structure put us in a centralized-like context moreover trees don't have cycles and, as said before, we found that this is a good property; hence, due to these considerations, we believe that trees are the most significant structure to analyze.

Switching leader signal

In this scenario we are going to perform some tests on a tree changing each time the reference value imposed by the leader node: step, ramp and sine wave and also changing the architecture so firstly with a neighborhood observer and secondly with a local observer; so that it is possible to appreciate the difference between them.

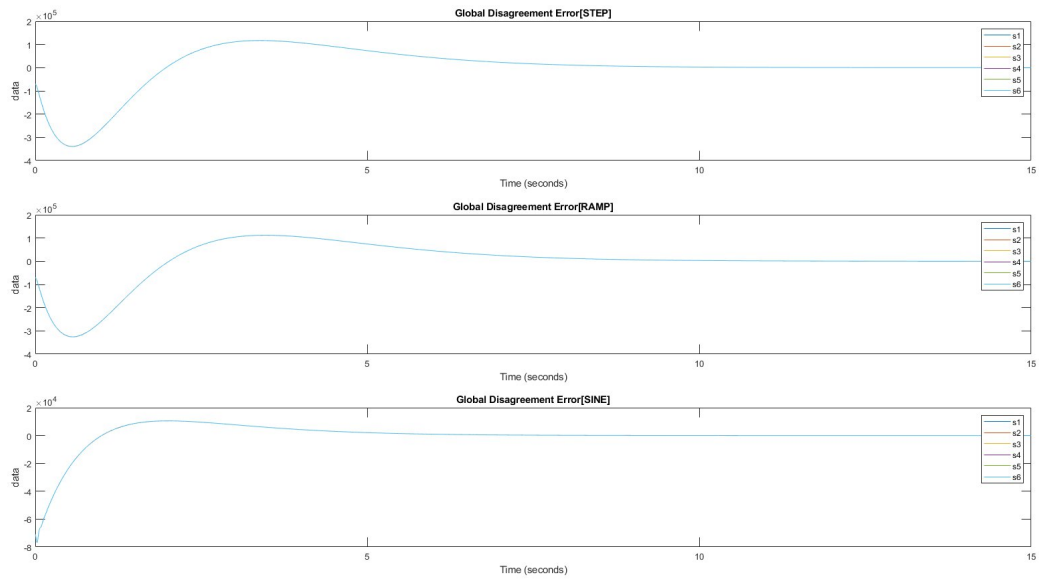
Distributed regulator based on a distributed neighborhood observer

The outcomes of our tests, based on our metrics, are the following and they took into consideration all the three scenarios.

The configuration used for testing both the architectures is: $R = Q = 1$ and a threshold = 100 (to find convergence time)

Signal type	SCT	CACT	ACO
Step	11.210	89.999	1,2,3,4,5,6
Ramp	11.504	89.998	1,2,5,4,6,3
Sine-wave	5.954	89.995	3,4,5,6,1,2

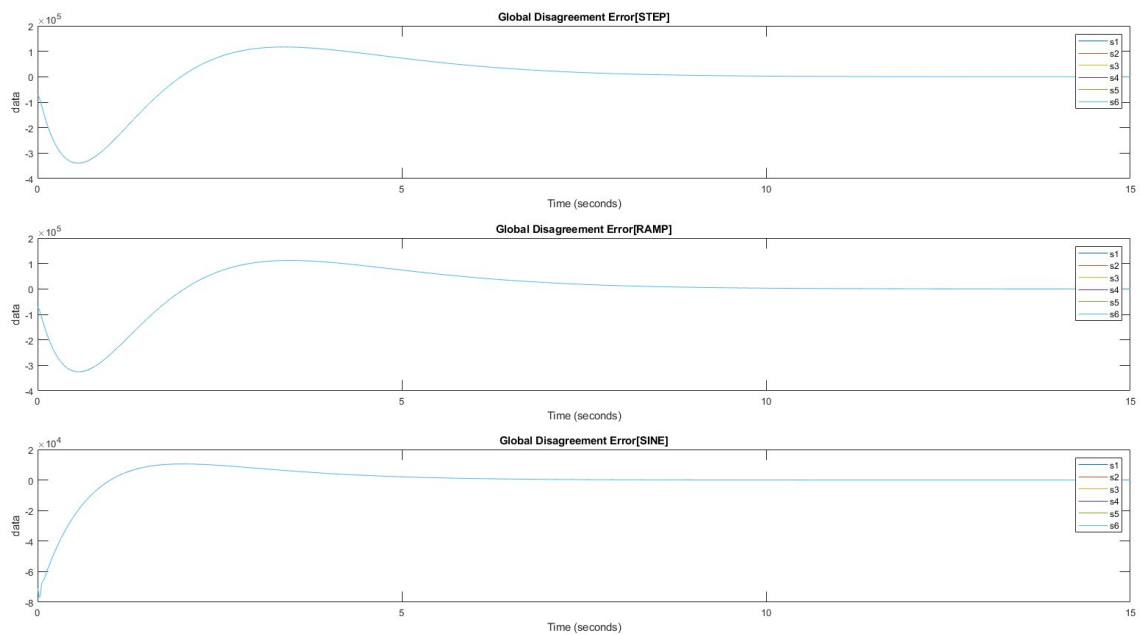
Global Disagreement Error (GDE)



Distributed regulator based on local observers

Signal type	SCT	CACT	ACO
Step	11.215	89.999	1,2,3,4,5,6
Ramp	11.450	89.997	1,2,3,4,5,3
Sine-wave	5.954	89.994	3,4,5,6,1,2

Global Disagreement Error (GDE)



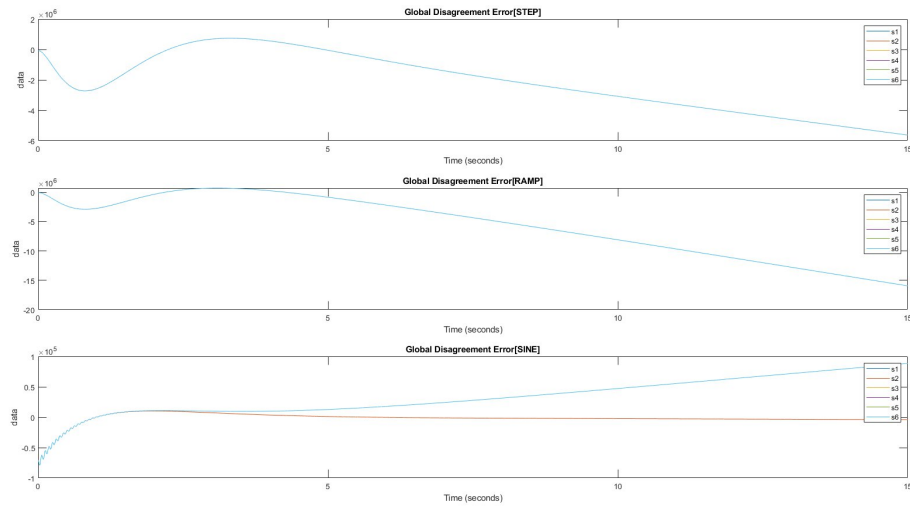
As known from the theory we expect the two architectures to have the same convergence time and it can be seen from these plots.

Effects of Measurement noises

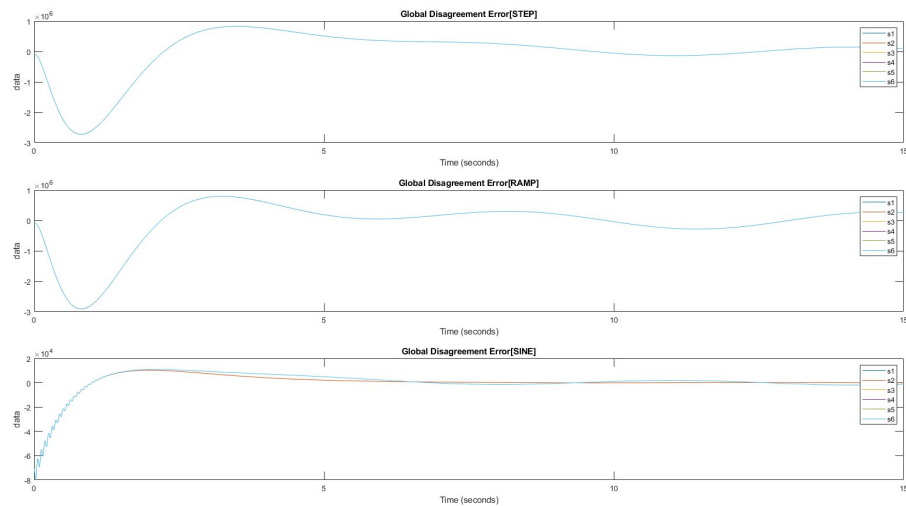
In order to perform these set of tests we decided to let c, Q and R in the default configuration ($Q=1$, $R=1$ and multiplicative factor of $c=10$) and we changed the topology of error in the following fashion:

Ramp error

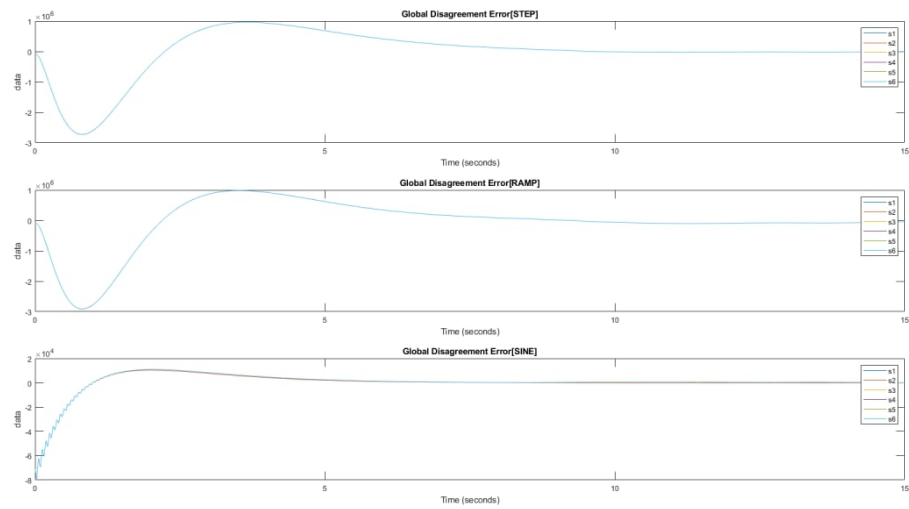
In this case we expect the system to diverge since the error increase in time



Sine error

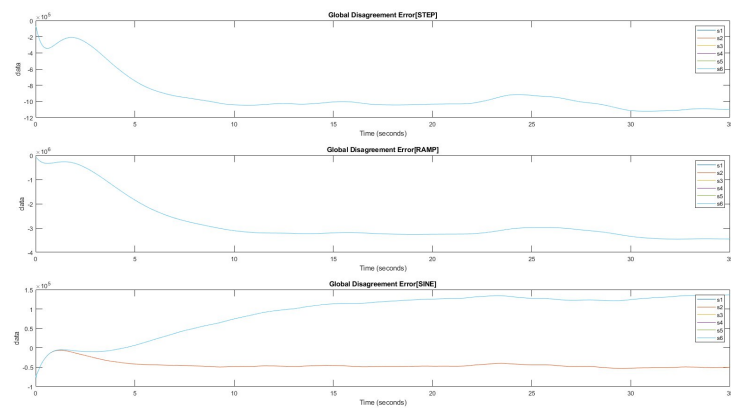


Random error

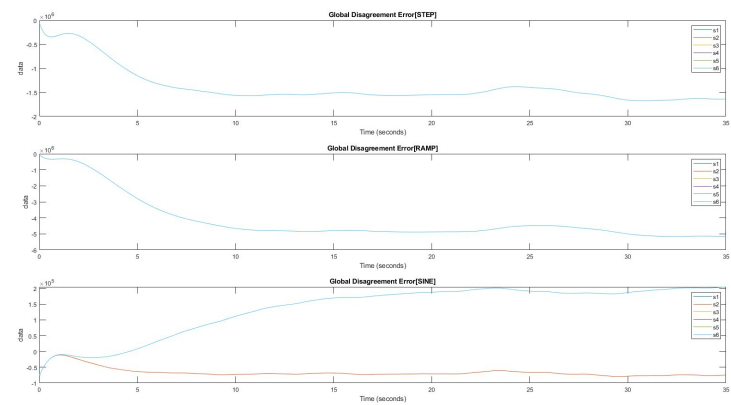


We also decided to show the robustness of the system changing the amplitude of the random error.

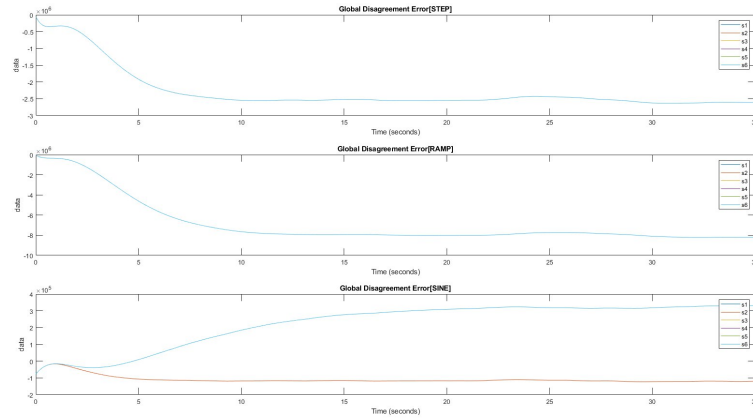
Mean 2 variance 1



Mean 3 variance 2



Mean 5 var 1

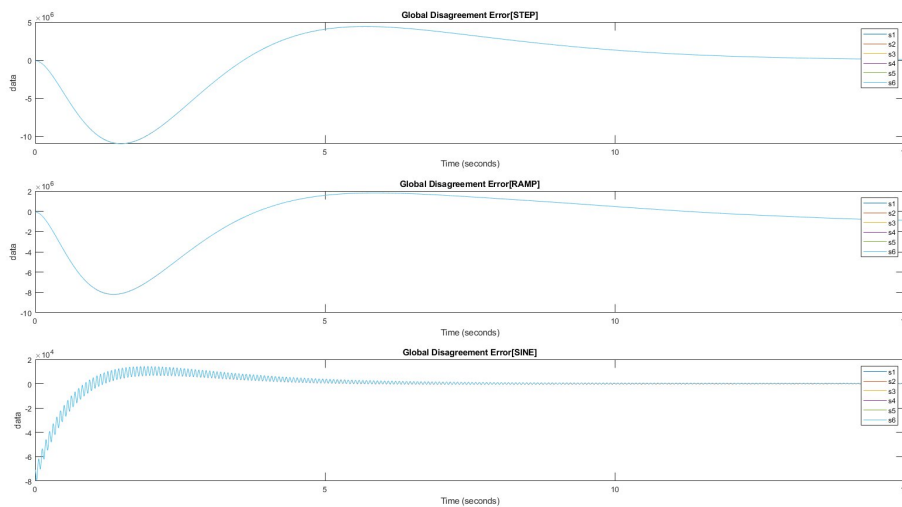


As it is possible to see there is no case in which we reach convergence so we can say that the control used it is not so robust.

Effect of matrices Q e R

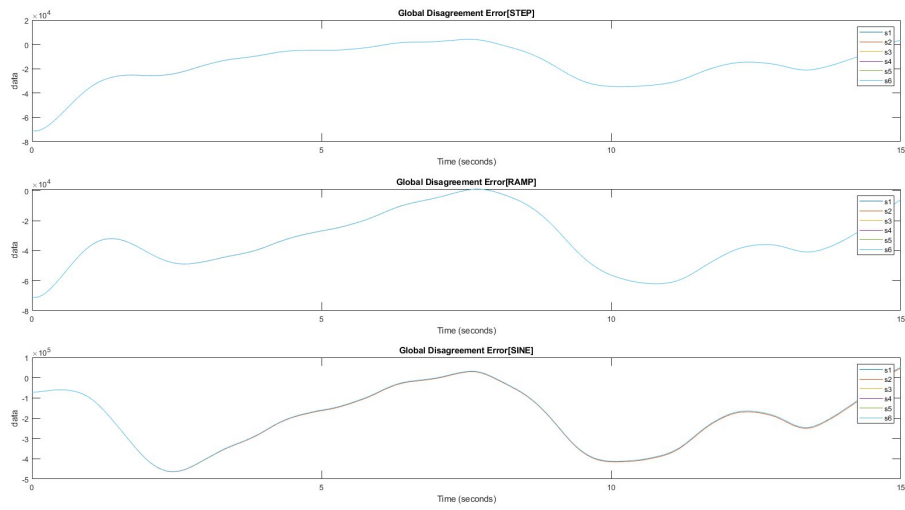
In order to perform these set of tests we decided to change c, Q and R in particular cases using a random noise.

$$R = 1000 \quad Q = 0.1$$

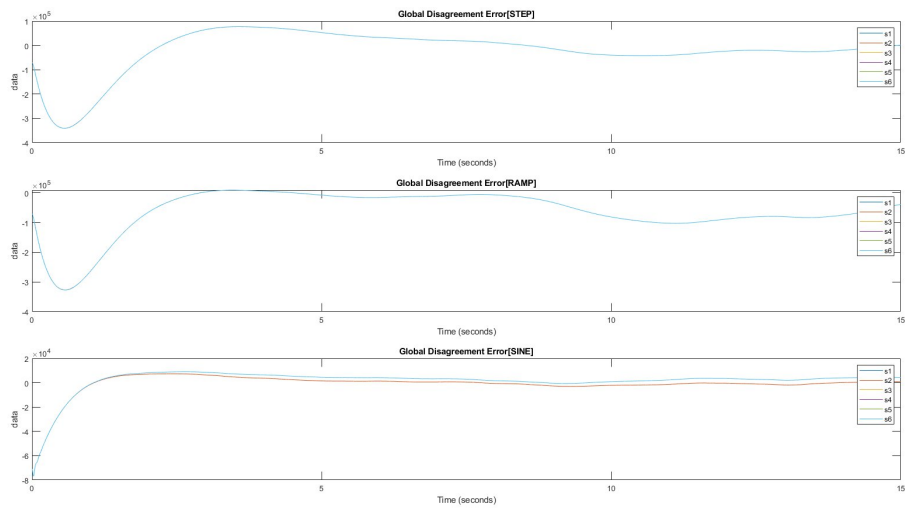


Having this configuration we would expect to have a worst performance with respect to a configuration with a higher Q and a minimized energy command signal.

$Q = 1000$ $R=0.1$

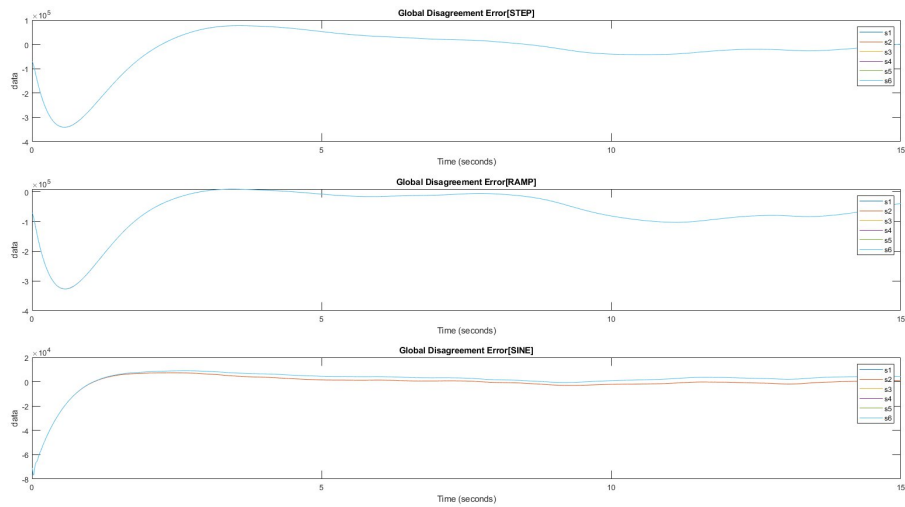


$R = 1000$ $Q = 1000$



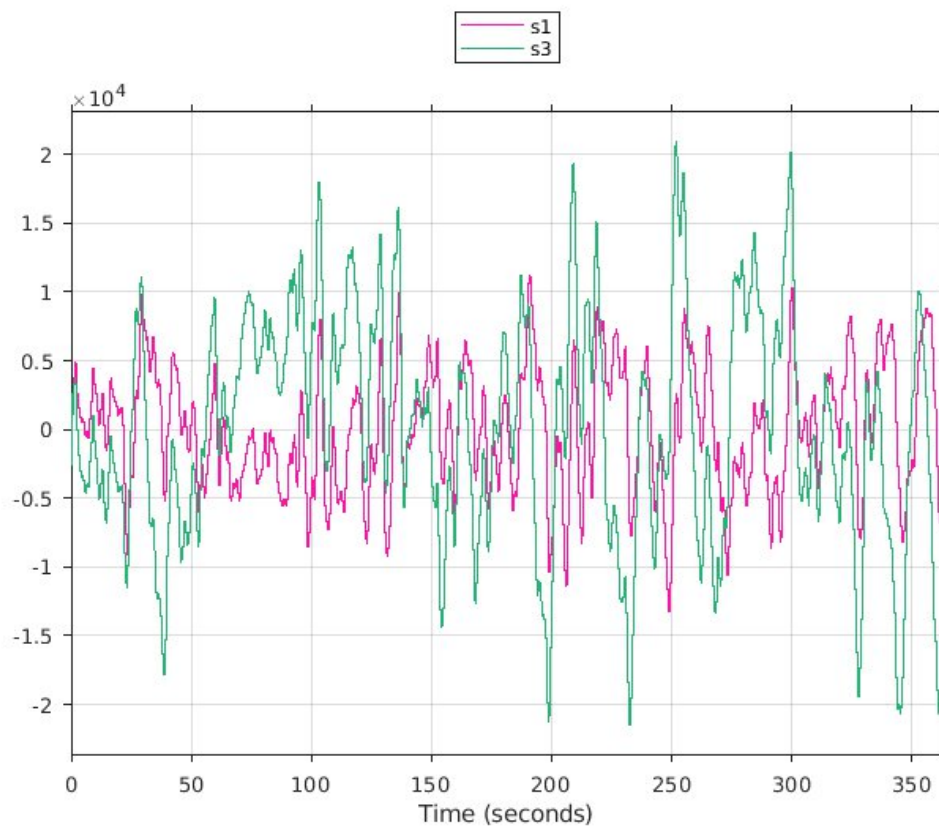
In this case, with a higher Q , we actually increased the performance of the system since the order of magnitude of the error is decreased.

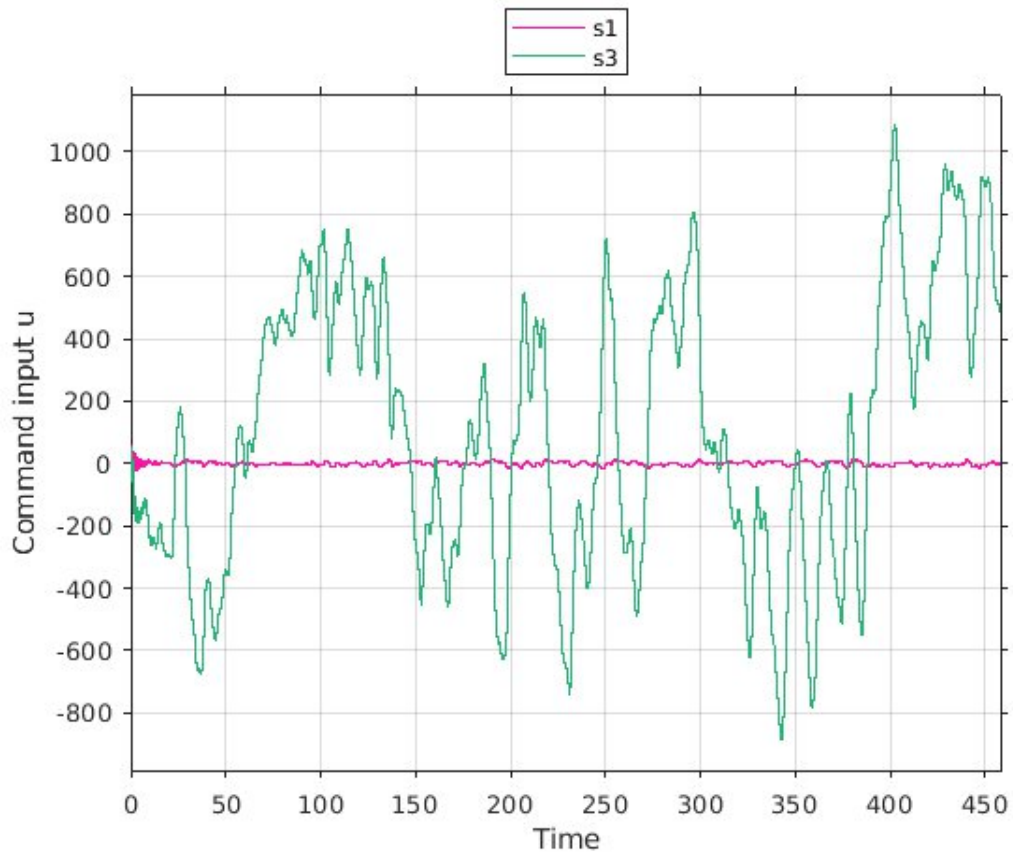
$Q = 0.1$ $R = 0.1$



As expected this configuration has a behavior analogous to the one $Q=1000$, $R=1000$ since their ratio is the same.

To better understand the preceding comments about R and the energy of the signal, we show the following plots:



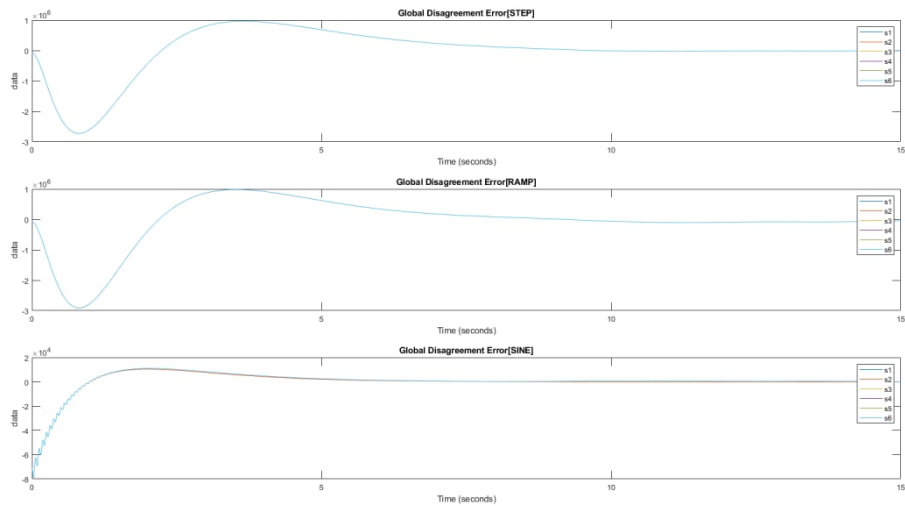


It is clear from the first plot ($R=0.1$) that the command input is not minimized while in the second plot ($R=1000$) this happen, indeed these two plots show a completely different order of magnitude. Moreover we plotted the command input of two nodes at two different depths and this allows us to see, regardless the value of R , the much higher effort that a node more distant from the leader has to face compared to a closer one.

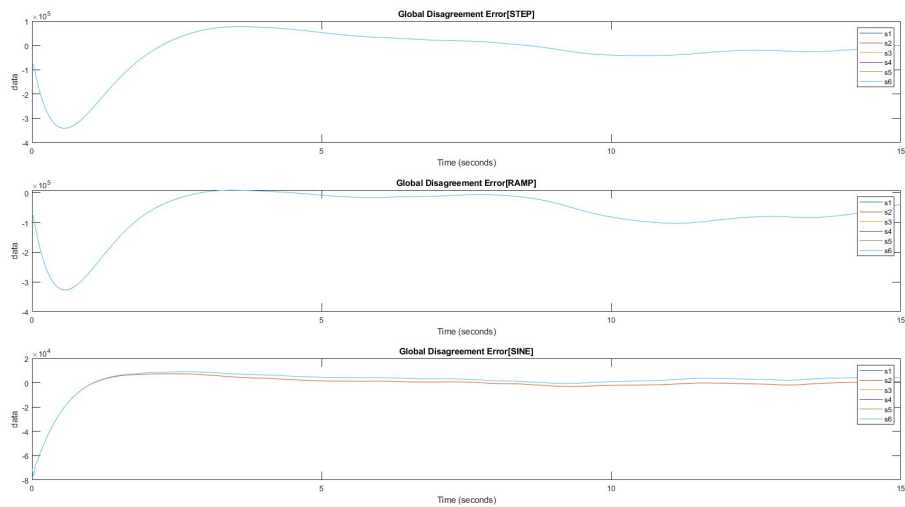
Effect of coupling gain

Now we decided to keep fixed Q and R to one and changed the multiplicative factor of c.

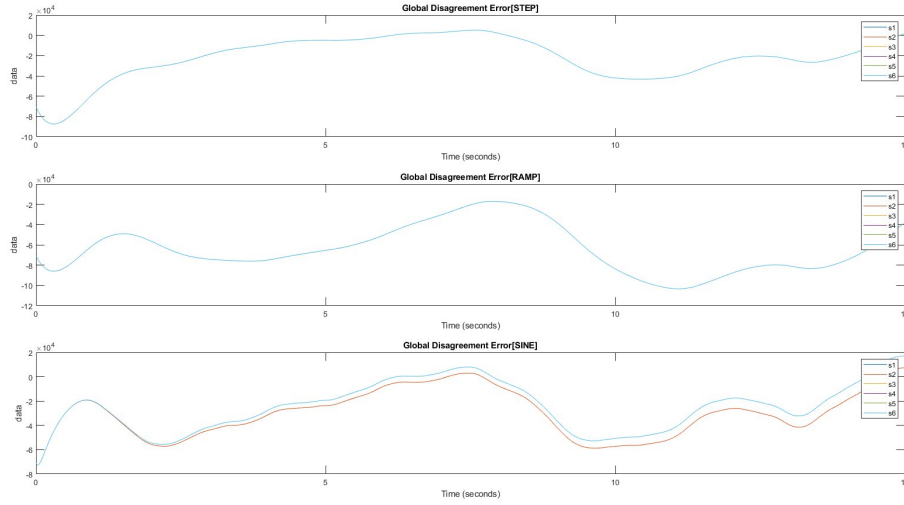
Numerator equals 1



Numerator equals 10



Numerator equals 100



In the case of a multiplicative factor of 100 and a sine signal reference we can see that nodes at depth 2 from the leader have a delay in convergence with respect to nodes closer and this is also due to the weights of the graph that are also the eigenvalues of the laplacian matrix.

Modified theory

Initially we wanted to control the maglev using the observer given by the theory. The problem was that the observer estimates only the state of the stabilized system, making it useless for our purposes. Through trial and error, we reached a point such that the estimation was the one we expected. We shall now explain this fact from a mathematical point of view.

We have the following system:

$$\begin{cases} \dot{x} = Ax + Bu \\ y = Cx \end{cases}$$

We define K^\star using the pole placement method, such that

$$\begin{cases} \dot{x} = Ax + Bu \\ u = -K^\star x + r \end{cases}$$

is stable.

Defining $A' = A - BK^\star$

Following the theory, we design a controller K as explained by theory.

$$K = R^{-1}B^TP$$

where P is the solution to the Algebraic Riccati Equation

$$A'P + PA'^T + Q - PB^TR^{-1}BP = 0$$

Finally, and this is where we made our modification, we define the observer as follows

$$F = PC^T R^{-1}$$

where P solves

$$AP + PA^T + Q - PB^T R^{-1} BP = 0$$

The point here is that we are using A instead of A' .

Using Theorem 3.2, we can show that the system converges using the Lyapunov equation

$$(A - c\lambda_i FCP) + P(A - c\lambda_i FC)^* = -Q - (2c\alpha_i - 1)FRF^T$$

to find that $M_o = A - c\lambda_i FCP$ is Hurwitz for each i .

The problem to conclude the proof was to find some kind of relationship between eigenvalues A and the eigenvalues of F and eventually with the eigenvalues of M_i .

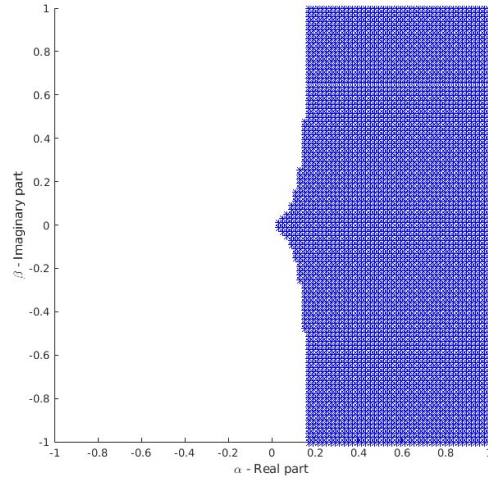
To conclude, we show the equations for each agent.

$$\begin{cases} \dot{x}_i = Ax_i + Bu_i \\ u_i = cK\epsilon_i - K^* \hat{x} \\ \epsilon_i = g_i(\hat{x}_0 - \hat{x}_i) + \sum_{j=1}^N a_{ij}(\hat{x}_j - \hat{x}_i) \\ \dot{\hat{x}}_i = A\hat{x}_i + Bu_i - cF\zeta_i \end{cases}$$

Where

$$\begin{cases} \zeta_i = g_i(\tilde{y}_0 - \tilde{y}_i) + \sum_{j=1}^N a_{ij}(\tilde{y}_j - \tilde{y}_i) \\ \tilde{y}_i = y_i - \hat{y}_i \\ y_i = Cx_i \\ \hat{y}_i = C\hat{x}_i \end{cases}$$

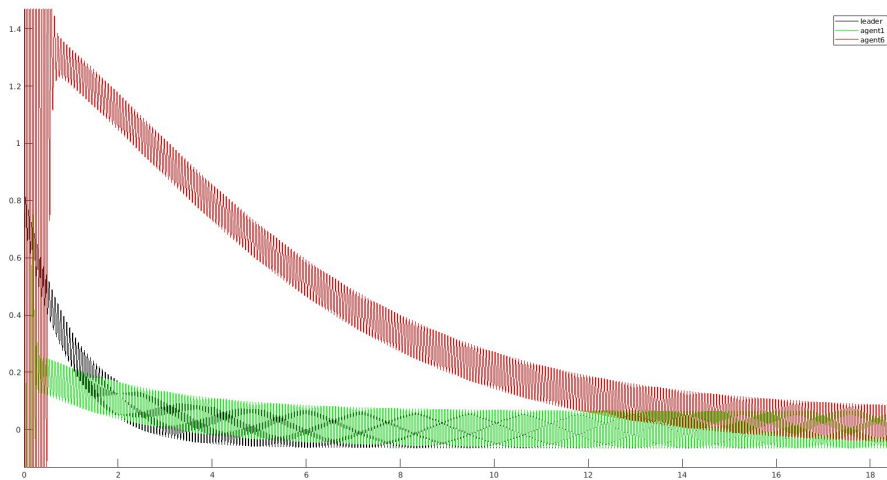
We analyzed such a system and computed the Synchronization Region. The following figure shows the synchronization region for the observed system (A, C) .

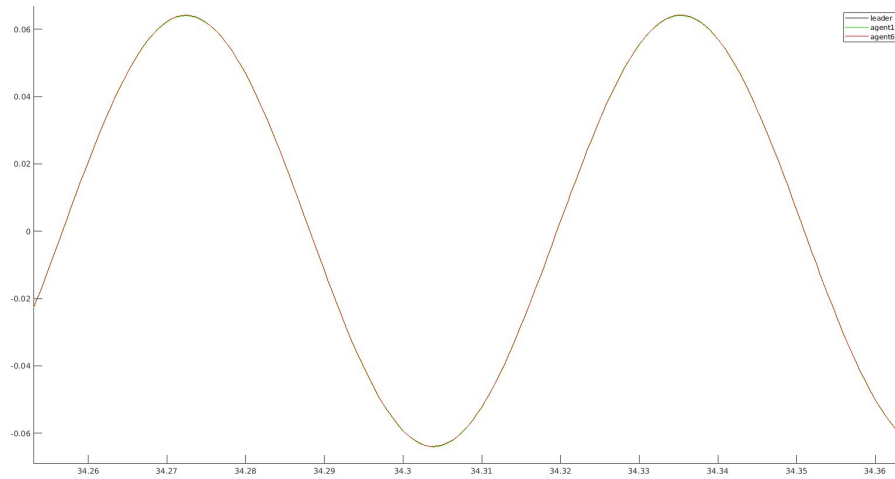


This plot shows us, under the conditions we designed the controller and the observer, the system converges.

This is surely a particular case, but this new method assures the existence of some conditions on A such that this architecture is stable.

We performed a simulation with the configuration just explained and the results is visible in the following figure.





The simulation was performed with a sinusoidal command reference with frequency $\omega = 100 \text{ rad/s}$. The convergence time is considered as the first last time the error $|y_i - y_0|$ is less than 1%.

Node	Convergence time (s)
1	7.68
2	10.83
3	13.49
4	16.00
5	18.44
6	20.86

The nodes were connected in a chain, because this result was obtained during the early phase of the project. The GDE is also order of magnitude smaller then the one in the other cases, since thi system only requires one observer.

